where

$$C_{mr} = \frac{1}{d}\int_0^d \cos\frac{r\pi y}{b}\cos\frac{m\pi y}{d}\,dy \quad (14)$$

$\Delta_m = 2$ if $m = 0$, $\Delta_r = 2$ if $r = 0$, and $\Delta_m = \Delta_r = 1$ otherwise and finally letting the subscripts o, e, c, and t have the same significance as applied to both a_{nr} and b_{nr} (but for the fact that even summation includes $r = n = 0$), we find that the cutoff frequencies of various modes may be deduced by solving the following equations

$$TE_{2n+1,2m+1}: \det[b_{nr(oc)}] = 0 \quad (15)$$

$$TE_{2n+1,2m}: \det[b_{nr(ee)}] = 0 \quad (16)$$

$$TE_{2n,2m+1}: \det[b_{nr(ot)}] = 0 \quad (17)$$

$$TE_{2n,2m}: \det[b_{nr(et)}] = 0. \quad (18)$$

Evidently (10) to (12) and (16) to (18) may be used to study modes in single-ridge waveguides; (16) and (18) are, with some changes in notation, due to Collins and Daly [5].

It can be shown that the cutoff frequencies of all modes reduce to those of the rectangular waveguide as the dimensions of the inner conductor tend to zero. Thus, for example, for $TM_{2n+1,2m}$ modes we note that when $2d/b = 1$, then for all s (including $s = 0$) we have $p_{1r} = p_{2m}$, $K_{mr} = K_{mn} = \frac{1}{2}$ subject to $n = r = m$. Hence (10) reduces to

$$\left[\coth p_{1r}\frac{s}{2a} + \tanh p_{1r}\left(\frac{1}{2} - \frac{s}{2a}\right)\right] \times \text{const.} = 0 \quad (19)$$

which has a solution

$$\coth\frac{p_{1r}}{2} = 0 \quad (20)$$

and hence

$$\lambda_c = 2/\sqrt{\left(\frac{2n+1}{a}\right)^2 + \left(\frac{2m}{b}\right)^2}$$

$$n = 0, 1, 2, \cdots, \quad m = 1, 2, \cdots. \quad (21)$$

Equations (20) and (21) hold for $TE_{2n+1,2m}$ modes as well subject to $m = 0, 1, 2, \cdots$.

Similarly, when $TM_{2n,2m+1}$ and $TE_{2n,2m+1}$ modes are considered, we find that the plane $s = 0$ represents an electric wall and hence, for all values of $2d/b$, the determinant vanishes when

$$\tanh\frac{p_{1r}}{2} = 0 \quad (22)$$

and

$$\lambda_c = 2/\sqrt{\left(\frac{2n}{a}\right)^2 + \left(\frac{2m+1}{b}\right)^2}. \quad (23)$$

With reference to the curves when $s = 0$, for the TE_{01} mode $\lambda_c/a = 1.6$ and for the TM_{21} mode $\lambda_c/a = 0.848$.

Furthermore, $TM_{2n,2m}$ and $TE_{2n,2m}$ modes have two planes of symmetry $s = 0$ and $2d/b = 1$ and hence (22) applies in conjunction with

$$\lambda_c = 2/\sqrt{\left(\frac{2n}{a}\right)^2 + \left(\frac{2m}{b}\right)^2}. \quad (24)$$

Specifically, when $s = 0$, for the TE_{20} mode $\lambda_c/a = 1$ and for the TM_{22} mode $\lambda_c/a = 0.625$.

Finally, $TE_{2n+1,2m+1}$ and $TM_{2n+1,2m+1}$ modes have no planes of symmetry. When $s = 0$ and $2d/b = 1$ determinants (10) and (15) diverge; however, in practice when $2d/b = 1$, $b/a = 0.8$ and $s = 0.03$, numerical computations reveal the presence of a root $\lambda_c/a = 1.249$ while for the rectangular waveguide corresponding to $s = 0$, $2d/b = 1$, we find that $\lambda_c/a = 1.249$ as well.

When $d = 0$ and $s = a$, the coaxial structure is transformed into two waveguides and the equations cannot be expected to hold in general.

However, a study of the field pattern suggests that when s approaches a, in the limit the ratio λ_c/a of a coaxial TE_{11} mode tends to that of a TE_{10} mode in a rectangular waveguide, viz., $\lambda_c/a = 2$; similarly, λ_c/a of the coaxial TE_{12} mode tends to that of a TE_{11} mode in a rectangular waveguide of reduced height (when $b/a = 0.8$, $2d/b = 0.6$, replacing b by $0.3b$ we find that $\lambda_c/a = 0.466$) etc. Numerical calculations confirm these conjectures.

The convergence with respect to m in both (8) and (13) is quite rapid and both expressions vary asymptotically as $0(m^{-3})$. Furthermore, the cutoff frequencies are primarily determined by a single diagonal term of $\det[a_{nr}]$ or $\det[b_{nr}]$ and a 3×3 determinant is likely to be adequate for most purposes.

It is of interest to note that the above procedure entails no approximations other than those inherent in the assumption that the walls are lossless. Normalized cutoff wavelength ratios λ_c/a obtained by Pyle [6] for the TE_{10} mode ($b/a = 0.45$) were compared with those obtained by the evaluation of 2×2 and 3×3 determinants of (16) and truncating the summation with respect to m after 8 terms. Typical results are shown below.

d/b	s/a	2×2 Determinant	3×3 Determinant	Reference [6]
0.2	0.2	3.769	3.920	3.985
0.2	0.9	2.892	2.916	2.961
0.8	0.2	2.121	2.140	2.163
0.8	0.9	2.051	2.051	2.057

Some λ_c/a characteristics of a rectangular coaxial waveguide (such that $b/a = 0.8$, $2d/b = 0.6$) are presented in Fig. 1.

An examination of these curves shows that as the frequency is increased and the propagation of higher-order modes becomes possible, the TE_{10} (TE_{01}) mode appears followed by the TE_{11} and TE_{20} modes (the TM_{11} mode precedes the TE_{20} mode for some combinations of $2d/b$ and s/a subject to the same aspect ratio $b/a = 0.8$); it also shows under what conditions two modes have the same cutoff frequency and hence velocity of propagation.

ACKNOWLEDGMENT

All computations were carried out on the Monash University CDC3200 computer.

L. GRUNER
Dept. of Elec. Engrg.
Monash University
Clayton, Victoria
Australia

REFERENCES

[1] O. R. Cruzan and R. V. Garver, "Characteristic impedance of rectangular coaxial transmission lines," *IEEE Trans. Microwave Theory and Techniques*, vol. MTT-12, pp. 488–495, September 1964.
[2] A. A. Oliner, "Theoretical developments in symmetrical strip transmission line," in *Proc. of the Symp. on Modern Advances in Microwave Techniques*, vol. 4. Brooklyn, N. Y.: Polytechnic Press of the Polytechnic Institute of Brooklyn, 1954.
[3] S. Hopfer, "The design of ridged waveguides," *IRE Trans. Microwave Theory and Techniques*, vol. MTT-3, pp. 20–29, October 1955.
[4] P. N. Butcher, "A theoretical study of propagation along tape ladder lines," *Proc. IEE* (London), pt. B, vol. 104, pp. 169–176, March 1957.
[5] J. H. Collins and P. Daly, "Orthogonal mode theory of single-ridge waveguides," *J. Electronics and Control*, vol. 17, pp. 121–129, August 1964.
[6] J. R. Pyle, "The cutoff wavelength of the TE_{10} mode in ridged rectangular waveguide of any aspect ratio," *IEEE Trans. Microwave Theory and Techniques*, vol. MTT-14, pp. 175–183, April 1966.

Numerical Solution of TEM-Line Problems Involving Inhomogeneous Media

Both empirical and analytical methods have been used in the past to evaluate the characteristic impedance of transmission lines supporting the TEM mode of wave propagation. Most of the analytical methods are rather tedious for practical use, employ approximations, or are restricted to simple configurations.

Therefore, in recent years, numerical methods for the solution of the Laplace equation in two dimensions in finite difference form using digital computers have been developed. From the Laplace equation, the potential distribution over the cross section of the transmission line is obtained, and integrating the potential gradient along a path enclosing the inner conductor yields the capacitance per unit length. This capacitance is used to determine the characteristic impedance and phase velocity of the line. Green[1] and Schneider[2] have investigated these procedures and used them to obtain interesting and useful results. For further information, these two papers or the numerous references cited in them should be consulted. The error involved in the assumption that a transmission line with inhomogeneous medium supports a pure TEM mode is a fraction of a percent up to frequencies of several gigahertz for configurations with similar dimensions to those under investigation in this correspondence.

With the use of integrated circuits on ceramic substrates suspended between two parallel ground planes, the knowledge of the characteristic impedance and phase velocity of such transmission lines in inhomogeneous media is necessary. The purpose of this correspondence is to investigate these two quantitites as a function of the various parameters defining the structure of the cross section.

The configuration which is discussed in this correspondence is shown in Fig. 1: two parallel ground planes with a spacing g between them. Centered between these ground

Manuscript received January 31, 1967; revised April 11, 1967.

[1] H. E. Green, "The numerical solution of some important transmission line problems," *IEEE Trans. Microwave Theory and Techniques*, vol. MTT-13, pp. 676–692, September 1965.
[2] M. V. Schneider, "Computation of impedance and attenuation of TEM lines by finite difference methods," *IEEE Trans. Microwave Theory and Techniques*, vol. MTT-13, pp. 793–800, November 1965.

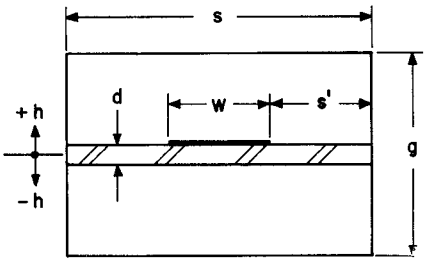

Fig. 1. Schematic cross section of TEM line.

planes is the ceramic substrate with the center conductor. The thickness of the substrate board is d, its dielectric constant ϵ_r. The width of the center conductor is w, its thickness is assumed to be zero (the actual value is about 0.5 mil). The sidewall spacing is s.

The standard dimensions of the transmission line under investigation are: $g=120$ mils and $d=24$ mils. The characteristic impedance Z and the normalized phase velocity v/v_0 were calculated as a function of w, ϵ_r, and sidewall to center conductor spacing s'. Small perturbations of the ground plane spacing g, of the vertical position of the dielectric board d and of its thickness h are also discussed.

Figure 2 shows Z and v/v_0 versus strip width w of the center conductor assuming a value of 8.0 for ϵ_r (typical for glazed alumina substrates) and sufficient sidewall spacing to prevent them from influencing the results. When w changes from 12 to 360 mils, Z varies between about 114 and 22 ohms, v/v_0 from 0.63 to 0.85. For $w=113$ mils, Z is 50 ohms and $v/v_0=0.77$. This corresponds to an effective dielectric constant $\epsilon_{eff}=1.67$. A 10 percent variation of w from the 50-ohm value causes a change of 6 percent of Z and a mismatch resulting in a VSWR of 1.06 (31 dB return loss). Stark from Bell Telephone Laboratories, Inc. obtained experimental results for Z for various values of w and for v/v_0 for $w=120$ mils. The ground-plane spacing of his configuration was $g=125$ mils. For comparison, these data are plotted in Fig. 2.

Next, the effect of sidewall spacing was investigated. Figure 3 shows Z and v/v_0 versus s', which is the distance between one sidewall and the nearest edge of the inner conductor; g is again 120 mils, $w=120$ mils, $d=24$ mils, and $\epsilon_r=8.0$. The impedance and phase velocity stay constant, i.e., independent of s' down to $s'=180$ mils. From there on Z and v decrease rapidly with decreasing s. In the constant region, the transmission line can be treated like a line with infinite sidewall spacing. All remaining calculations were done with sufficiently large s.

Figure 4 presents the dependence of Z and v/v_0 of the standard line ($g=w=120$ mils, $d=24$ mils) on the dielectric constant ϵ_r. ϵ_r is varied between 1 and 25. Correspondingly, Z varies from 63 ohms to about 41 ohms, v/v_0 from 1 to 0.65. There is a larger variation of Z and v in the region of small ϵ_r than for the higher ϵ_r values. An ϵ_r of 6.5 gives a 50-ohm line for the present choice of parameters, v/v_0 is 0.80. A 10 percent change of ϵ_r from 6.5 causes only about 1.5 percent impedance variation. The VSWR connected with this mismatch is only 1.01, the return loss therefore is larger than 45 dB.

Exact ground-plane spacing, centering of the dielectric board, and exact thickness of the board are important factors for the production of these transmission lines. Therefore, the dependence of Z and v on these parameters was also studied. The dependence of Z on g is

0.38 Ω/mil for the line width $w=72$ mils,
0.31 Ω/mil for the line width $w=120$ mils,
and
0.27 Ω/mil for the line width $w=192$ mils.

The impedance ratios of these three lines are like 1:0.76:0.56, the impedance versus g dependences are like 1:0.81:0.71, i.e., the impedances of low ohmic lines are somewhat more g dependent than higher ohmic lines.

From this, the necessary ground-plane spacing for a 50-ohm line turns out to be 125 mils with an ϵ_r of 8.0, $w=120$ mils, and $d=24$ mils.

The velocity change versus g is very small; it is actually smaller than the accuracy of the computed results.

Next, the vertical position of the dielectric board was varied 24 mils to both sides of the center position $h=0$. Again Z and v/v_0 were computed for the three lines with $w=72$, 120, and 192 mils strip widths as shown in Fig. 5.

It was found that there is a position of maximum Z which is about 6 mils below the center line for all three of the lines. In this position, small variations of the vertical position do not affect the impedance. The velocity variations over the 48-mil range of h are appreciable:

from 0.685 to 0.768 for line width $w=72$ mils,
from 0.716 to 0.816 for line width $w=120$ mils,
and
from 0.745 to 0.857 for line width $w=192$ mils.

The reason for this variation is the change in the distribution of electromagnetic energy over the cross section: when the board moves upwards, a larger percentage of energy concentrates between the center conductor and the upper ground plane, the dielectric between them is air, the velocity goes up. When the board moves down, more energy is concen-

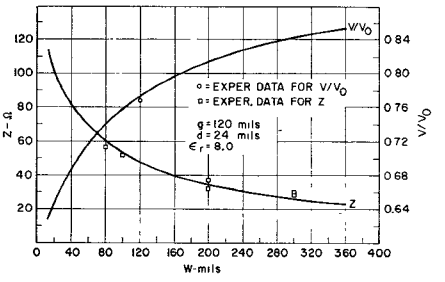

Fig. 2. Z and v/v_0 versus width w of the center conductor for $g=120$ mils, $d=24$ mils, and $\epsilon_r=8$. (Experimental results for $g=125$ mils.)

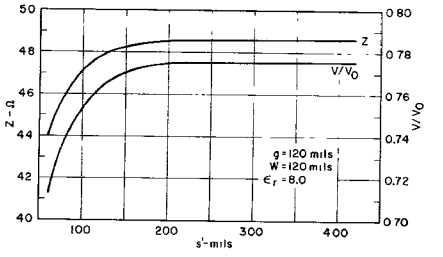

Fig. 3. Z and v/v_0 versus sidewall spacing s' with $g=120$ mils, $w=120$ mils, $d=24$ mils, and $\epsilon_r=8$.

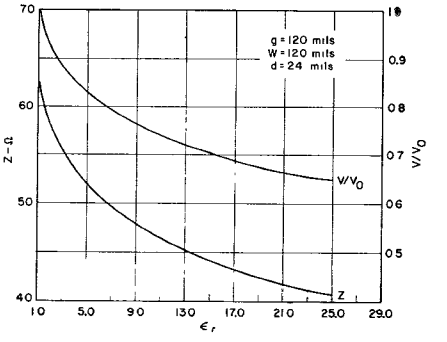

Fig. 4. Z and v/v_0 versus dielectric constant ϵ_r with $g=120$ mils, $w=120$ mils, and $d=24$ mils.

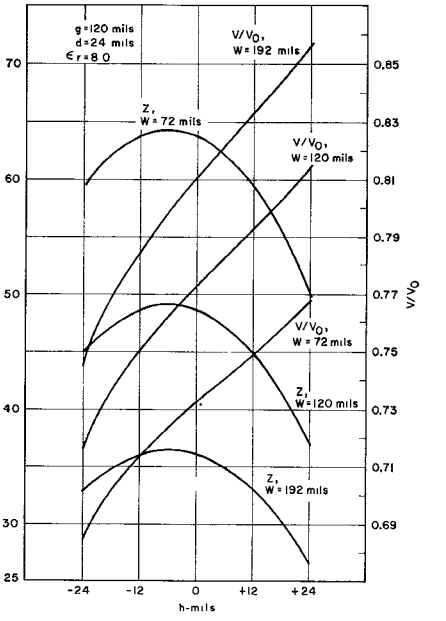

Fig. 5. Z and v/v_0 versus vertical deviation h from center position of dielectric board for lines with $w=72$, 120, and 192 mils with $g=120$ mils, $d=24$ mils, and $\epsilon=8$.

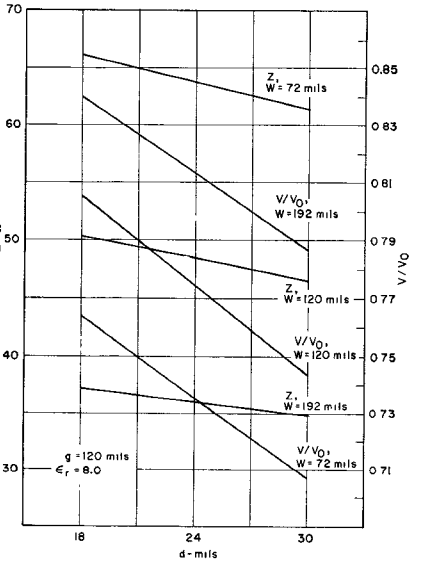

Fig. 6. Z and v/v_0 versus thickness of dielectric board d for lines with $w=72$, 120, and 192 mils with $g=120$ mils and $\epsilon_r=8$.

trated between center conductor and lower ground plane, i.e., in the dielectric board, and the velocity goes down.

Finally, the thickness of the dielectric board was changed, again for the three preceding lines. The positions of the center conductor and of the upper edge of the board were kept constant, and the thickness was varied by changing the location of the lower edge of the board. The results for d values of $d=18$, 24, and 30 mils are shown in Fig. 6. The impedance and phase velocity decrease as expected with increasing thickness.

The impedance slope of these curves indicates a Z versus d dependence of

0.39 Ω/mil for the line width $w=72$ mils,
0.32 Ω/mil for the line width $w=120$ mils,
and
0.19 Ω/mil for the line width $w=192$ mils.

As the impedance ratios of the three lines are 1:0.76:0.56 and the Z versus d dependences are 1:0.82:0.49, it follows that a change in d is about equally critical for lower and higher ohmic lines within the range of consideration.

The fractional velocity variation is the same as the fractional impedance variation.

The accuracy of these calculations for Z is typically around 1 percent but not worse than 2 percent, for v/v_0 typically around 0.5 percent but not worse than 1 percent.

ACKNOWLEDGMENT

The author wishes to thank K. Kurokawa for useful advice during the progress of the work.

H. E. BRENNER
Bell Telephone Labs., Inc.
Holmdel, N. J.

Realizations of a Duo-Pole Branch of an Elliptic-Function Bandstop Filter

This correspondence illustrates six realizations of the TEM line (transformed) equivalent of the LC network A of Fig. 1. Network A is here taken to represent a shunt branch of a low-pass elliptic-function ladder filter [1]. Richards' transformation [2] converts a lumped element low-pass filter to a transmission-line bandstop filter [3]–[6]. Each filter element, L or C, is then replaced by a short- or open-circuited quarter-wave stub. Thus, network A is transformed to network B, with parameters as defined in Fig. 1. The six stripline and reentrant slabline networks C-H are equivalent to network B and are well suited for microwave filters. The characteristic impedances of the lines in networks C, D, E, and H are given in Fig. 1, and the coupled-line impedances of networks F and G are given in Schiffman and Matthaei [5] and Schiffman [7]. Although networks F and G are shown as cascaded sections [5], [7] (not duo-pole type), here they are shunt-connected with the far terminals open circuited. In networks B-D, line Z_1 is short circuited and line Z_2 is open circuited at its far end, and lines Z_1 and Z_2 are in series with each other at their near ends. In networks E and H, Z_2' is open circuited and in cascade with Z_1'.

Manuscript received March 23, 1967.

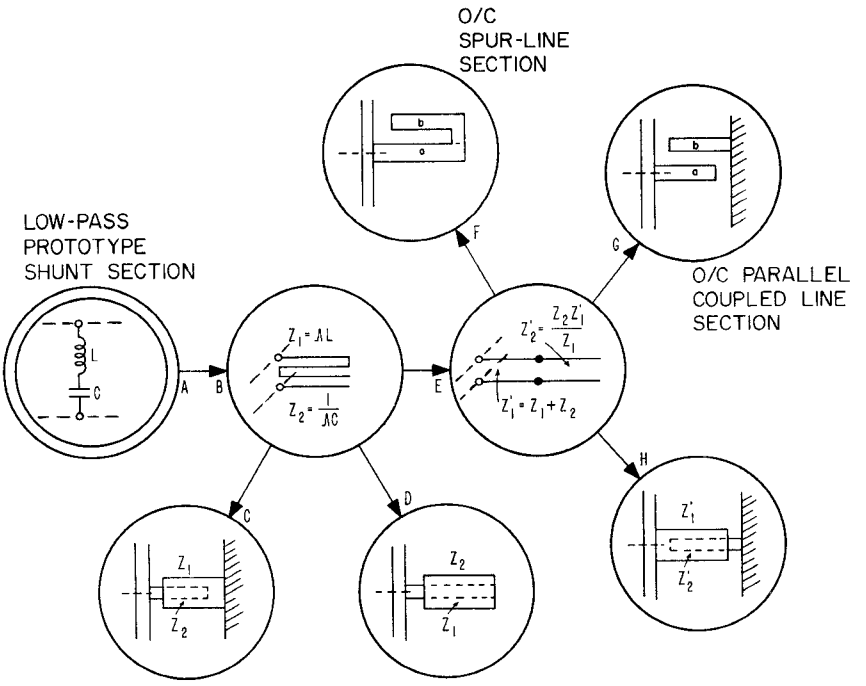

Fig. 1. Stripline and reentrant slabline realizations of a shunt duo-pole branch of an elliptic-function bandstop filter. Here, $\Lambda=\omega_1'\tan[(\pi/2)(\omega_0-\omega_1)/\omega_0)]$ where ω_1 and ω_1' are corresponding frequencies (usually taken as band-edge frequencies) in the bandstop and low-pass frequency domains, and ω_0 is center of stopband.

B. M. SCHIFFMAN
Stanford Research Inst.
Menlo Park, Calif. 94025

REFERENCES

[1] R. Saal and E. Ulbrich, "On the design of filters by synthesis," *IRE Trans. Circuit Theory*, vol. CT-5, pp. 284–327, December 1958.
[2] P. I. Richards, "Resistor-transmission-line circuits," *Proc. IRE*, vol. 36, pp. 217–220, February 1948.
[3] H. Ozaki and J. Ishii, "Synthesis of transmission-line networks and the design of UHF filters," *IRE Trans. Circuit Theory*, vol. CT-2, pp. 325–336, December 1955.
[4] A. I. Grayzel, "A synthesis procedure for transmission-line networks," *IRE Trans. Circuit Theory*, vol. CT-5, pp. 172–181, September 1958.
[5] B. M. Schiffman and G. L. Matthaei, "Exact design of band-stop microwave filters," *IEEE Trans. Microwave Theory and Techniques*, vol. MTT-12, pp. 6–15, January 1964.
[6] R. J. Wenzel, "Exact design of TEM microwave networks using quarter-wave lines," *IEEE Trans. Microwave Theory and Techniques*, vol. MTT-12, pp. 94–111, January 1964.
[7] B. M. Schiffman, "Two nomograms for coupled-line sections for band-stop filters," *IEEE Trans. Microwave Theory and Techniques (Correspondence)*, vol. MTT-14, pp. 297–299, June 1966.

Characteristic Impedance of Multifin Transmission Lines

Several years ago, the author had occasion to investigate the characteristic impedance properties of a TEM transmission line of unusual cross section. Specifically, the cross section consisted of a round outer conductor with a center conductor composed of a number of thin fins symmetrically positioned about the axis of the line. Examples of this general class of cross section are illustrated in Fig. 1 for the cases of two, three, four, and six fins. Solutions for the characteristic impedances of this type of configuration were obtained by an interesting series of conformal transformations that mapped the multifin line geometry into that of a symmetric strip transmission line. Since the characteristic impedance of the latter is well known, curves can readily be generated for the multifin line impedance.

The basic steps in the mapping process are outlined in Fig. 2. First, geometries having other than two fins are mapped into the two-fin case by applying the transformation

$$z' = z^{n/2} \tag{1}$$

where n is the number of fins in the given geometry (z plane). Since this transformation maps $2/n$ of the multifin line space into the entire space of the two-fin line, the effect will be to establish the relations

$$Z_n = \frac{2}{n} Z_2 \tag{2}$$

when

$$\frac{r_n}{R_n} = \left(\frac{r_2}{R_2}\right)^{2/n} \tag{3}$$

where Z_n, r_n, R_n and Z_2, r_2, R_2 are the characteristic impedance, fin radial dimension, and shield radius of the n-fin and two-fin lines, respectively. Note that the z and z' planes are normalized so that the shield lies on the unit circle.

Manuscript received March 16, 1967.